

Nonequilibrium dynamics of the localization-delocalization transition in non-Hermitian Aubry-André model

Liang-Jun Zhai^{1,2}, Guang-Yao Huang³, and Shuai Yin^{4*}

¹*Department of Physics, Nanjing University, Nanjing 210093, China*

²*The school of mathematics and physics, Jiangsu University of Technology, Changzhou 213001, China*

³*Institute for Quantum Information & State Key Laboratory of High Performance Computing, College of Computer Science and Technology, National University of Defense Technology, Changsha 410073, China and*

⁴*School of Physics, Sun Yat-Sen University, Guangzhou 510275, China*

(Dated: May 26, 2022)

In this paper, we investigate the driven dynamics of the localization transition in the non-Hermitian Aubry-André model with the periodic boundary condition. Depending on the strength of the quasi-periodic potential λ , this model undergoes a localization-delocalization phase transition. We find that the localization length ξ satisfies $\xi \sim \varepsilon^{-\nu}$ with ε being the distance from the critical point and $\nu = 1$ being a universal critical exponent independent of the non-Hermitian parameter. In addition, from the finite-size scaling of the energy gap between the ground state and the first excited state, we determine the dynamic exponent z as $z = 2$. The critical exponent of the inverse participation ratio (IPR) for n th eigenstate is also determined as $s = 0.1197$. By changing ε linearly to cross the critical point, we find that the driven dynamics can be described by the Kibble-Zurek scaling (KZS). Moreover, we show that the KZS with the same set of the exponents can be generalized to the localization phase transitions in the excited states.

I. INTRODUCTION

The quasi-periodic system, lying in between the periodic system and the disordered system, exhibits very interesting properties, such as the topological phase [1–6], the Anderson localization [7–14], the quantized adiabatic pumping [3, 15], and the cascade of the localization transition [16]. As a typical model, the Aubry-André (AA) model [7, 17], whose on-site potential has an irrational period compared with the lattice period, has received increasing attention in recent years, partly inspired by its realization in the pseudorandom optical lattice [18], and ultracold atoms [19]. It was shown that the AA model can undergo a localization transition with the change of potential strength [5, 7, 12, 13], in contrast to the case of the disordered system which only has the localization phase in one dimension [20–22]. Moreover, various extensions of AA models have been studied. For example, the energy-dependent mobility edges is found in a generalized AA model with modified quasiperiodic potentials [9] and long-range hopping terms [10, 11], and the critical phase lying between the extended and localized phase is found for a generalized AA model with two quasiperiodic modulation parameters [15, 23, 24], and many-body localization (MBL) has been found in the AA model with the interaction term introduced [24–28].

Recently, nonequilibrium dynamics in localized systems has attracted increasing attentions. Lots of exotic properties therein have been discovered. For instance, it is shown that the periodic driving can not only turn the localized eigenstates into extended ones and vice versa [29, 30], but also bring the system into the topo-

logical MBL phase [31]. In addition, a dynamical localization transition can happen when the system is suddenly quenched from the localized phase to the delocalized phase [32, 33]. Furthermore, for the linearly quench across the localization transition point, the driven dynamics can be well described by the Kibble-Zurek scaling (KZS) [34].

On the other hand, inspired by the experimental progress, the non-Hermitian systems have attracted enormous studies [35–54]. In particular, it has been shown that the interplay of non-Hermiticity and the disordered (or quasi-periodic) potentials can bring intriguing perspectives in the localization phenomena [2, 55–83]. For instance, it was shown that for the non-Hermitian AA model with the non-reciprocal hopping the localization transition happens at the same point as the real-complex transition [2, 58, 61, 68, 84]. For the nonequilibrium dynamics in non-Hermitian localization systems, the periodical driving and the sudden quench have been studied [85–88]. However, linearly quench dynamics in the localization transition in the non-Hermitian systems is still unexplored. A natural question is whether the KZS is still applicable in describing the driven dynamics in the localization transition in the non-Hermitian systems.

To answer this question, in the present paper we study the scaling behavior of the driven dynamics of localization transition in the non-Hermitian AA model [58]. The non-Hermiticity of this model is induced by the non-reciprocal hopping. According to the locations of the critical points of the localization-delocalization transition and real-complex transition, we classify the eigenstates into three classes. The first class is the ground state, in which the energy spectrum is always real and this type of the state has only the localization transition. The second class corresponds to the eigenstates in which the localization transition and real-complex transition hap-

* yinsh6@mail.sysu.edu.cn

pen at different points. The third class corresponds to the eigenstates in which the localization transition and real-complex transition happen at the same critical point. Then, we study the driven dynamics in this model for various kinds of states. Starting from the deep localized phase and slowly tuning the potential strength across the critical point, we find that the driven dynamics of the localization-delocalization phase transition for different types of initial state can be described by the KZS. Accordingly, we generalize the KZS to localization transition in the non-Hermitian quasi-periodic systems.

The remainder of the paper is organized as follows. In Sec. II, the non-Hermitian AA model is introduced, and the static scaling behaviors are presented. In Sec. III, the driven dynamics of the localization-delocalization transition is studied. The KZS for various kinds of states is examined by the numerical study. A summary is given in Sec. IV.

II. NON-HERMITIAN AA MODEL AND THE STATIC CRITICAL PROPERTIES

A. The non-Hermitian AA model

The Hamiltonian of the non-Hermitian AA model reads [58]

$$H = - \sum_i^L (J_L C_j^\dagger C_{j+1} + J_R C_{j+1}^\dagger C_j) + 2\lambda \cos [2\pi(\gamma j + \phi)] C_j^\dagger C_j, \quad (1)$$

where $C_j^\dagger (C_j)$ is the creation (annihilation) operator of the hard-core boson, $J_L = J e^{-g}$ and $J_R = J e^g$ are the asymmetry hopping amplitude in the left and right directions, respectively, λ measures the amplitude of the quasi-periodic potential with γ therein being an irrational number, and $\phi \in [0, 1)$ is a random phase of the potential. The periodic boundary condition is assumed in the following calculation. To satisfy the periodic boundary condition, γ has to be approximated by a rational number F_n/F_{n+1} where $F_{n+1} = L$ and F_n are the Fibonacci numbers. It was shown that all the eigenstates of model (1) are localized when $\lambda > e^g$, while all the eigenstates are delocalized when $\lambda < e^g$. Thus the critical point for the localization transition is $\lambda_c = e^g$ [58, 62].

As illustrated in Fig. 1, the energy spectrum of Eq. (1) are plotted. Here, the eigenstates are arranged in a descending order of the real parts of the eigenenergies. We find that the eigenstates can be classified into three classes. Class I: The first class has the real spectra for all λ . The typical states in this class is the ground state. Class II: The second class corresponds to the states in which the real-complex transition and the localization transition happen at different λ . The second type eigenstates usually locate at the boundary of the energy bands, i.e., the red curves in Fig. 1. Class III: The third class is

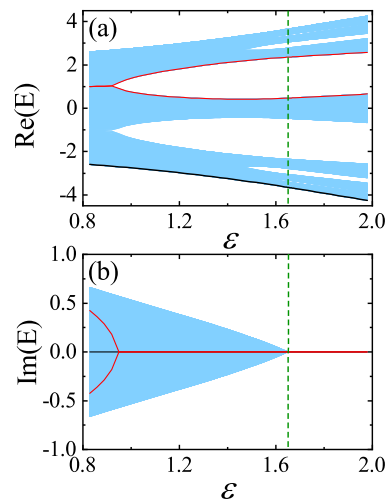


FIG. 1. (a) Real and (b) imaginary parts of energy spectra of the model Eq. (1). The black curve is the ground state belonging to Class I. The red curves denote the eigenstates belonging to Class II with the localization transition and real-complex transition being separated. The blues curves denote the third type of eigenstates belonging to Class III with localization transition and real-complex transition happening at the same critical point. Here, we choose $g = 0.5$, $\phi = 0$ and $L = 987$ in the calculation. The green dashed lines in (a) and (b) label the location of the localization transition critical point.

the eigenstate that undergoes a real-complex transition at $\lambda = \lambda_c$ accompanying with the localization transition. We find that most of the excited eigenstates belong to the this class.

B. Static scaling properties for localization transition

Here we systematically explore the scaling properties of the localization transition for three kinds of spectra. For the ground state in Class I, three quantities can be used to characterize the localization transition. One is the localization length, ξ , defined in the localization phase as [34]

$$\xi = \sqrt{\sum_{n>n_c}^L [(n - n_c)^2] P_i}, \quad (2)$$

in which P_i is the probability of the wavefunction at site i , $n_c \equiv \sum n P_i$ is the localization center. Near the localization-delocalization transition, for $\varepsilon \equiv \lambda - \lambda_c$, it is expected that ξ satisfies the scaling relation

$$\xi \propto \varepsilon^{-\nu}, \quad (3)$$

when $\xi \ll L$.

The second quantity is the inverse participation ratio (IPR) for n th eigenstate, which is defined as [58, 89, 90]

$$\text{IPR}_n = \frac{\sum_{j=1}^L |\Psi_n^R(j)|^4}{\sum_{j=1}^L |\Psi_n^R(j)|^2}, \quad (4)$$

where $|\Psi_n^R(j)\rangle$ is the n th right eigenvector. For the extended state with $\lambda < \lambda_c$, the wave function is homogeneously distributed through all sites, and $\text{IPR}_n \propto L^{-1}$, while for the localization state with $\lambda > \lambda_c$ $\text{IPR}_n \propto L^0$. At the localization transition point λ_c , it is expected that IPR_n satisfies a scaling relation

$$\text{IPR}_n \propto L^{-s/\nu}, \quad (5)$$

with s being its exponent. When $L \rightarrow \infty$, s can also be determined by

$$\text{IPR}_n \propto \varepsilon^s. \quad (6)$$

The third quantity is the energy gap between the first excited state and the ground state. According to the finite-size scaling, this energy gap Δ_s should scales as

$$\Delta_s \propto L^{-z}, \quad (7)$$

when $\lambda = \lambda_c$.

For Class II and Class III, the energy gap that is relevant to the localization transition cannot be well-defined. But the scaling relations of the localization length Eq. (3) and the IPR_n Eqs. (5-6) can also be used to characterize the localization transition in the excited states. A peculiar situation for Class III is that the real-complex spectra phase transitions happens at the same point as the localization transition. However, the real-complex spectra transition and the localization transition are described by different universality classes. For the former, as λ decreases, a pair of real energy levels converge as $\Delta_r \propto \varepsilon_r^{1/2}$ in which $\varepsilon_r = \lambda - \lambda_r$ is the distance from the real-complex transition point λ_r , and Δ_r is the energy difference between these two energy level for $\varepsilon_r > 0$; while for $\varepsilon_r < 0$ a pair of complex energy levels generate with the same real-part of energy and their imaginary-parts of the energies satisfy $\Delta_i \propto |\varepsilon_r|^{1/2}$ in which Δ_i denotes the imaginary-parts of the energy difference. Thus, for this transition, the critical exponent $\nu_r z_r = 1/2$. This behavior is characterized by the (0 + 1)D Yang-Lee edge singularity [91–93]. In contrast, in the following, we will show that for the localization transition, $\nu z = 2$.

In the following, we will numerically examine Eqs. (3-7) and determine ν , s and z . The numerical results of the ξ of the ground state for different g are shown in Fig. 2 (a). For Class I, Fig. 2 (a) confirms the scaling relation of Eq. (3) and demonstrates that $\nu = 1$. Moreover, the results for different g displayed in Fig. 2 (a) demonstrate that ν is a universal exponent independent of g . In addition, Fig. 2 (b) shows that IPR_n in the localization transition in the ground state satisfies Eq. (5) and

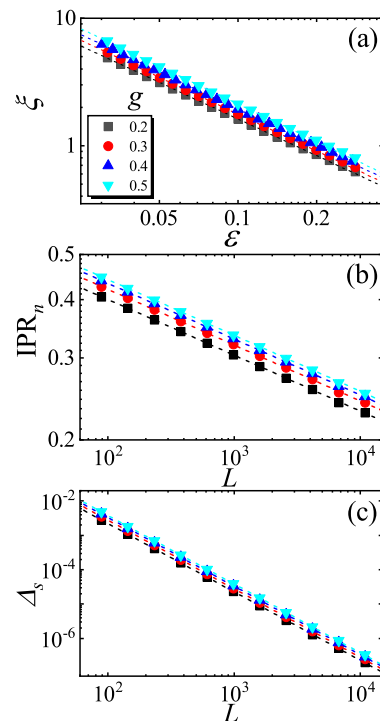


FIG. 2. Static scaling properties in the ground state. (a) Curves of localization length ξ versus ε for $L = 987$, (b) IPR_n at $\lambda = \lambda_c$ versus L , and (c) Energy gap Δ_s at $\lambda = \lambda_c$ versus L for different g . Here, the results are averaged for 100 choices of ϕ . The power law fitting yields $\nu = 0.9557, 0.9631, 0.9719$ and 0.9803 , and $s = 0.1196, 0.1197, 0.1198$ and 0.1198 and $z = 1.995, 1.998, 1.997$ and 1.997 , for $g = 0.2, 0.3, 0.4$ and 0.5 , respectively.

the averaged critical exponent $s = 0.1197$, which is consistent with the result in a non-Hermitian interpolating Aubry-André-Fibonacci model [62]. Moreover, Fig. 2 (c) shows that the energy gap at the critical point satisfies $\Delta_s \propto L^z$ with $z = 2$. Note that this value is different from the one obtained for the localization transition in Hermitian Hamiltonian, where $z = 2.37$ [22, 34, 94].

For Class II and Class III, we calculate the localization length and show the results in Figs. 3 (a) and (c). These results demonstrates that the localization length in the excited state also satisfies Eq. (3) with $\nu = 1$. In addition, we calculate the IPR_n for the localization transition in the states belonging to Class II and Class III. Figs. 3 (b) and (d) show that IPR_n at the localization transition for both cases satisfy $\text{IPR}_n \propto \varepsilon^{0.1294}$ and $\text{IPR}_n \propto \varepsilon^{0.1201}$, similar to the case of Class I. These results indicate that the localization transitions for all three classes of states belong to the same universality class. In the next section, we will show that the dynamic exponent for both Class II and III is $z = 2$, although it cannot be determined via the gap scaling.

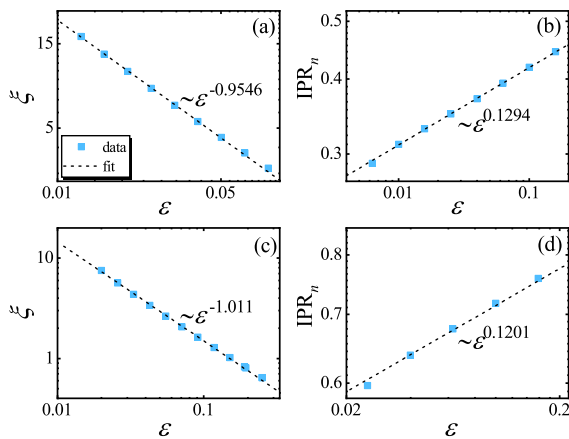


FIG. 3. Static scaling properties in different kinds of excited states. ξ versus ε for (a) the 609th eigenstate (Class II) and (c) the third eigenstate (Class III). IPR_n versus ε for (b) the 609th excited eigenstate (Class II) and (d) the third excited eigenstate (Class III). Here, we use $L = 2584$ and $g = 0.5$. The results are averaged for 100 choices of ϕ .

III. KIBBLE-ZUREK SCALING IN THE NON-HERMITIAN AA MODEL

A. General theory of the KZS

In usual phase transitions, when the tuning parameter ε is changed linearly as

$$\varepsilon = -Rt, \quad (8)$$

to drive a system cross its critical point, the KZS states that for $|\varepsilon| > R^{1/\nu r}$ with $r = z + 1/\nu$ the system can evolve adiabatically since the state has enough time to adjust to the change of the Hamiltonian; while for $|\varepsilon| < R^{1/\nu r}$ the system enters the impulse region and ceases to evolve as a result of the critical slowing down. However, investigations showed that the assumption that the system stop evolving in the impulse region is quite excessive. For instance, a finite-time scaling theory demonstrates that in the impulse region the system evolves according to a time scale $\zeta \sim R^{-z/r}$ [95–97]. Accordingly, for a quantity Y , its full scaling form reads

$$Y(\varepsilon, R) = R^{y/r} f_Y(tR^{z/r}), \quad (9)$$

in which y is the critical exponent of Y and is defined according to the static scaling $Y \propto \varepsilon^y$ when $L \rightarrow \infty$, and f_Y is the scaling function. At the critical point, $t = 0$, Eq. (9) demonstrates that Y can be scaled with R as $Y \propto R^{y/\nu r}$ for $L \rightarrow \infty$. Equation (9) was first established in classical phase transitions [98–100]. In quantum phase transitions, similar scaling forms were also proposed from different perspectives in various systems [101–103]. Recently, the KZS and the full scaling form Eq. (9) have been generalized into the non-Hermitian Yang-Lee edge singularity [91, 104] and the localization transition in the

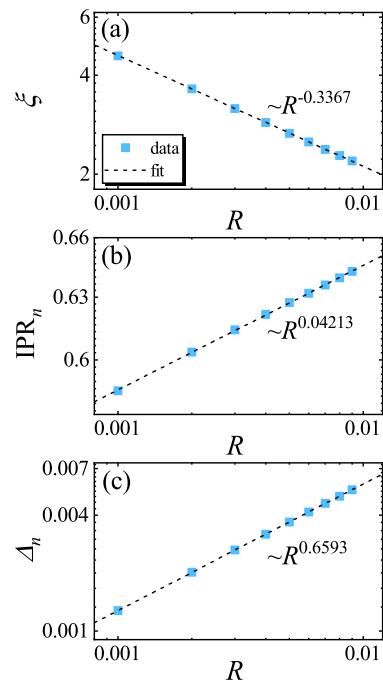


FIG. 4. (a) ξ and (b) IPR_n at $t = 0$ and (c) Δ_n at $tR^{z/r} = 0.5$ as a function of R for the initial ground state. Here, we use $g = 0.5$ and $L = 987$. The results are averaged for 10 choices of ϕ .

ground state of the Hermitian system [34, 105]. In the following, we will generalize this scaling form into the localization transition in the non-Hermitian AA model (1).

B. KZS in states of Class I

We at first explore the driven dynamics in the states in Class I. We focus on the driven dynamics in the ground state. In addition, we set the lattice size L very large and the finite-size effects can be ignored. For the localization length ξ , Eq. (9) converts to

$$\xi(t, R) = R^{-1/r} f_\xi(tR^{z/r}), \quad (10)$$

in which $r = 3$. Besides, according to Eq. (9), the dynamic scaling form of IPR_n is

$$\text{IPR}_n(t, R) = R^{s/r\nu} f_{\text{I}}(tR^{z/r}). \quad (11)$$

In addition, we define an energy difference $\Delta_n(t)$ between the time-dependent state and the n th eigenstate as

$$\Delta_n(t) \equiv \text{Re}[\langle \Psi_n^L(t) | H(t) | \Psi_n^R(t) \rangle - E_n], \quad (12)$$

where $\langle \Psi_n^L(t) | \equiv \langle \Psi_n^L(0) | e^{iH(t)t}$ and $|\Psi_n^R(t)\rangle \equiv e^{-iH(t)t} |\Psi_n^R(0)\rangle$, $|\Psi_n^R(0)\rangle$ and $\langle \Psi_n^L(0) |$ are the right and left eigenstates at the initial time, and E_n is the n th eigenenergy for the instantaneous Hamiltonian $H(t)$. The driven dynamics of Δ_n satisfy

$$\Delta_n(t, R) = R^{z/r} f_\Delta(tR^{z/r}), \quad (13)$$

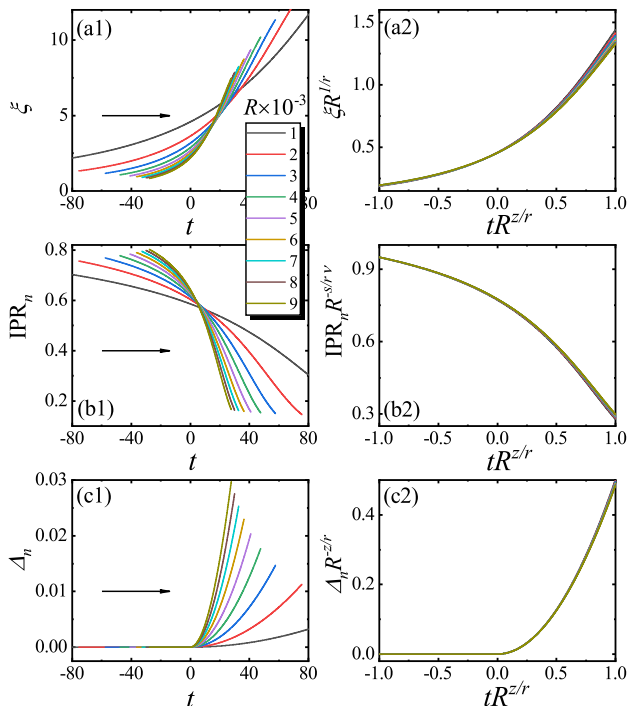


FIG. 5. Driven dynamics with the initial ground state. The curves of ξ versus t before (a1) and after (a2) rescaling for different R . The curves of IPR_n versus t before (b1) and after (b2) rescaling for different R . The curves of Δ_n versus t before (c1) and after (c2) rescaling for different R . Here, we use $g = 0.5$ and $L = 987$, the results is averaged for 10 choices of ϕ . The arrows in (a1), (b1) and (c1) point the quench direction.

according to Eq. (9).

Then, we numerically examine Eqs. (10), (11) and (13) for the states of Class I. First, we show in Fig. 4 (a) that at the localization transition point ξ satisfies $\xi \propto R^{-0.3367}$ in the ground state. The critical exponent is close to $-1/r$. Furthermore, by rescaling ξ and t as $tR^{z/r}$, one finds that the rescaled curves collapse onto each other for the ground state as shown in Fig. 5 (a1) and (a2), confirming Eq. (10). Second, Fig 4 (b) shows that at the critical point IPR_n obeys $\text{IPR}_n \propto R^{0.04213}$ for the ground state. Then, by rescaling IPR_n and t as $\text{IPR}_n R^{-s/r\nu}$ and $tR^{z/r}$, respectively, one finds that the rescaled curves collapse onto each other for the ground state as shown in Fig. 5 (b1) and (b2), confirming Eq. (11). Third, Fig 4 (c) shows that Δ_n obeys $\Delta_n \propto R^{0.6593}$ at $tR^{z/r} = 0.5$ for the ground state. Then, by rescaling Δ_n and t as $\Delta_n R^{-z/r}$ and $tR^{z/r}$, respectively, one finds that the rescaled curves collapse onto each other for the ground state as shown in Fig. 5 (c1) and (c2), confirming Eq. (11).

C. KZS in states of Class II and Class III

In this section, we will show that Eqs. (10), (11) and (13) are also applicable for localization phase transitions

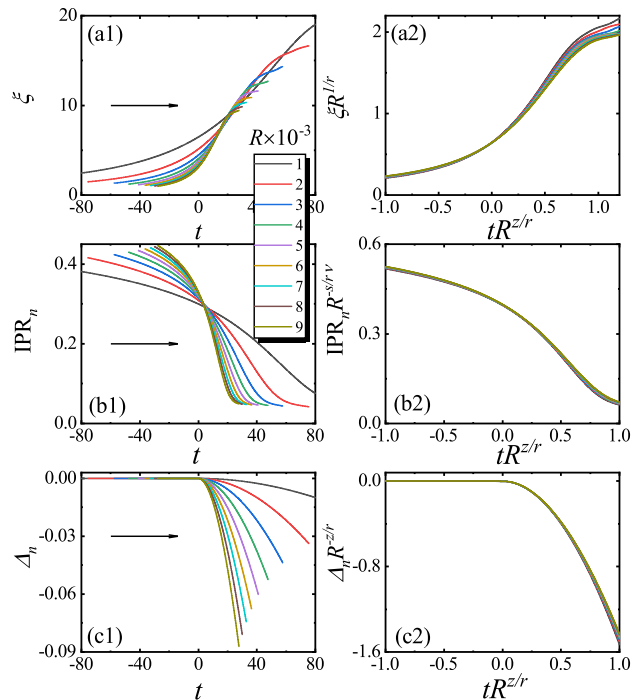


FIG. 6. Driven dynamics with the initial state belonging to Class II. The curves of ξ versus t before (a1) and after (a2) rescaling for different R . The curves of IPR_n versus t before (b1) and after (b2) rescaling for different R . The curves of Δ_n versus t before (c1) and after (c2) rescaling for different R . Here, we use $g = 0.5$ and $L = 987$. We choose 609th excited state as the initial state in the figure. The results is averaged for 10 choices of ϕ . The arrows in (a1), (b1) and (c1) point the quench direction.

in the states belonging to Class II and III. For the Class II state, the real-complex transition happens at smaller value of ε , comparing with the localization transition point. Accordingly, the localization transition happens at the the real-spectra region. Figures 6 (a1), (b1) and (c1) show the evolution of ξ , IPR_n and Δ_n , respectively, for 609th excited state. After rescaling according to Eqs. (10), (11) and (13) with the same set of the critical exponents, we find the rescaled curves collapse onto each other, as shown in Figs. 6 (a2), (b2) and (c2). These results confirm that the rescaling functions Eqs. (10), (11) and (13) are applicable for Class II eigenstates. In particular, for Δ_n , we find that it decreases as t increases, different from the case of the initial ground state, as shown in Fig. 5 (c1). The reason is that when the initial state is the ground state, the energy can only increase under external driving. In contrast, when the initial state is in the excited state, the energy can spread to both higher and lower states. In the present 609th excited state, the lower-energy excitation dominates, as shown in Figs. 6 (c1) and (c2).

For the Class III state, we choose the third excited state as an example. We calculate the evolution of ξ , IPR_n and Δ_n and show the results in Fig. 7. We find

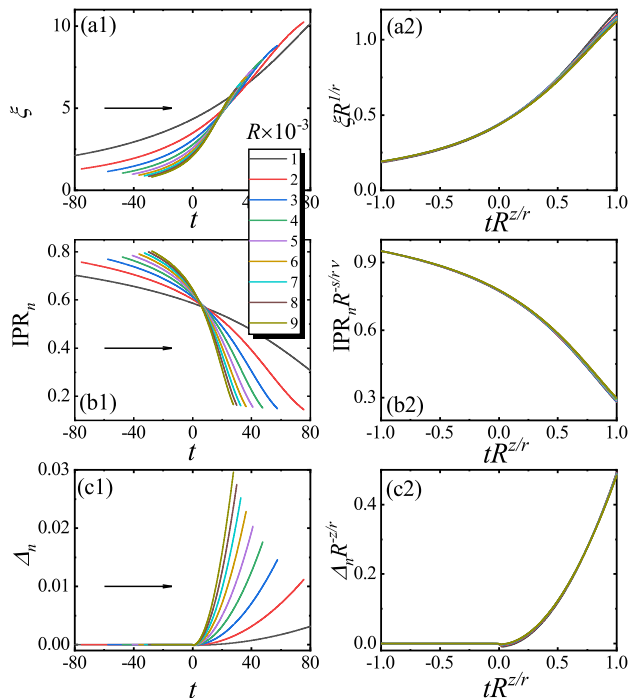


FIG. 7. Driven dynamics with the initial state belonging to Class III. The curves of ξ versus t before (a1) and after (a2) rescaling for different R . The curves of IPR_n versus t before (b1) and after (b2) rescaling for different R . The curves of Δ_n versus t before (c1) and after (c2) rescaling for different R . Here, we use $g = 0.5$ and $L = 987$. The third excited state is taken as the initial state in the figure. The results is averaged for 10 choices of ϕ . The arrows in (a1), (b1) and (c1) point the quench direction.

that the rescaled curves, according to Eqs. (10), (11) and (13) with the same set of the critical exponents, collapse onto each other. These results confirm that the scaling functions Eqs. (10), (11) and (13) are applicable for Class III eigenstates.

For the Class III state, the real-complex transition happens at the same point as the localization transition. Since these two kinds of phase transitions belong to different universality classes, a nature question is whether the real-complex transition affects the universal scaling behavior. To answer this question, we compare the relevant exponents for these two transitions. For the scaling of the correlation length $\xi \sim R^{-1/r}$, the exponent

$-1/r$ is always $-1/3$ for both the localization transition and the real-complex transition. So the scaling of the correlation length satisfies the same scaling form for the real-complex transition and the localization transition. Accordingly, from the scaling of the correlation length, one cannot distinguish the contribution of the real-complex transition from that of the localization transition. For the energy scaling $\Delta_n \sim R^{z/r}$, the exponent z/r is $2/3$ for the localization transition but is $1/3$ for the real-complex transition. For small driving rate, it seems that the contribution from the real-complex transition can dominate. However, there are only two relevant states for the real-complex transition. For instance, for the third state, only the fourth state is relevant. The energy gap of these two states vanishes at the transition point and becomes complex value in the other side of the transition point. However, for the localization transition, there are lots of states can be occupied under the external driving. Thus, the contribution from the localization transition will dominate. This argument is supported by the scaling of ξ shown in Fig. 7 (c).

IV. SUMMARY

In summary, we have studied the driven dynamics of the non-Hermitian AA model. We have first determined the static exponent ν , s and z by investigating the static behavior of ξ , IPR_n and Δ_s , respectively. Then we have studied the driven dynamics of the localization-delocalization transitions for three classes of states. We have found that the driven dynamics in all of these states can be described by the KZS with the same set of critical exponents. Our paper generalizes the KZS to the localization transition in both the ground state and the excited states in non-Hermitian systems.

ACKNOWLEDGMENTS

We thank A. Sinha for helpful discussions. L.-J. Zhai is supported by China Postdoctoral Science Foundation (Grant No. 2021M691535) and the National Natural science Foundation of China (Grant No. 11704161). S. Yin is supported by the National Natural science Foundation of China (Grant No. 41030090).

-
- [1] M. Verbin, O. Zilberberg, Y. E. Kraus, Y. Lahini, and Y. Silberberg, Observation of Topological Phase Transitions in Photonic Quasicrystals, *Phys. Rev. Lett.* **110**, 076403 (2013)
- [2] S. Longhi, Topological Phase Transition in non-Hermitian Quasicrystals, *Phys. Rev. Lett.* **122**, 237601 (2019).

- [3] Y.E. Kraus, Y. Lahini, Z. Ringel, M. Verbin, O. Zilberberg, Topological States and Adiabatic Pumping in Quasicrystals, *Phys. Rev. Lett.* **109**, 106420 (2012).
- [4] D.-W. Zhang, Y.-Q. Zhu, Y.X. Zhao, H. Yan, S.-L. Zhu, Topological quantum matter with cold atoms, *Adv. Phys.* **67**, 253-402 (2018).
- [5] S. Ganeshan, K. Sun and S. Das Sarma, Topological Zero-Energy Modes in Gapless Commensurate Aubry-

- André-Harper Models, *Phys. Rev. Lett.* **110**, 180403 (2013).
- [6] L.-J. Lang, X. Cai, and S. Chen, Edge States and Topological Phases in One-Dimensional Optical Superlattices, *Phys. Rev. Lett.* **108**, 220401 (2012).
- [7] S. Aubry and G. André, Analyticity breaking and Anderson localization in incommensurate lattices, *Ann. Israel Phys. Soc.* **3**, 133 (1980).
- [8] J.B. Sokoloff, Band structure and localization in incommensurate lattice potentials, *Phys. Rev. B* **23**, 6422-6429 (1981).
- [9] S. Das Sarma, S. He, X.C. Xie, Mobility Edge in a Model One-Dimensional Potential, *Phys. Rev. Lett.* **61**, 2144-2147 (1988).
- [10] J. Biddle, B. Wang, D. J. Priour, and S. Das Sarma, Localization in one-dimensional incommensurate lattices beyond the Aubry-André model, *Phys. Rev. A* **80**, 021603 (2009).
- [11] J. Biddle, D.J. Priour, B. Wang, S. Das Sarma, Localization in one-dimensional lattices with non-nearest-neighbor hopping: Generalized Anderson and Aubry-André models, *Phys. Rev. B*, **83**, 075105 (2011).
- [12] H. P. Lüschen, S. Scherg, T. Kohlert, M. Schreiber, P. Bordia, X. Li, S. Das Sarma, and I. Bloch, Single-Particle Mobility Edge in a One-Dimensional Quasiperiodic Optical Lattice, *Phys. Rev. Lett.* **120**, 160404 (2018).
- [13] S. E. Skipetrov and A. Sinha, Time-dependent reflection at the localization transition, *Phys. Rev. B* **97**, 104202 (2018).
- [14] U. Agrawal, S. Gopalakrishnan and R. Vasseur, Universality and quantum criticality in quasiperiodic spin chains, *Nat. Commun.* **11**, 2225 (2020).
- [15] F. Liu, S. Ghosh, Y.D. Chong, Localization and adiabatic pumping in a generalized Aubry-André-Harper model, *Phys. Rev. B* **91**, 014108 (2015).
- [16] V. Goblot, A. Štrkalj, N. Pernet, J. L. Lado, C. Dorow, A. Lemaître, L. Le Gratiet, A. Harouri, I. Sagnes, S. Ravets, A. Amo, J. Bloch and O. Zilberberg, Emergence of criticality through a cascade of delocalization transitions in quasiperiodic chains, *Nat. Phys.* **16**, 832-836 (2020).
- [17] P. G. Harper, Single Band Motion of Conduction Electrons in a Uniform Magnetic Field, *Proc. Phys. Soc. A* **68**, 874 (1955).
- [18] G. Roati, C. D'Errico, L. Fallani, M. Fattori, C. Fort, M. Zaccanti, G. Modugno, M. Modugno and M. Inguscio, Anderson localization of a non-interacting Bose-Einstein condensate, *Nature* **453**, 895-898 (2008).
- [19] J. Billy, V. Josse, Z. Zuo, A. Bernard, B. Hambrecht, P. Lugan, D. Clément, L. Sanchez-Palencia, P. Bouyer, A. Aspect, Direct observation of Anderson localization of matter waves in a controlled disorder, *Nature* **453**, 891-894(2008).
- [20] P. W. Anderson, Absence of Diffusion in Certain Random Lattices, *Phys. Rev.* **109**, 1492 (1958).
- [21] F. Evers and A. D. Mirlin, Anderson transitions, *Rev. Mod. Phys.* **80**, 1355 (2008).
- [22] B.-B. Wei, Fidelity susceptibility in one-dimensional disordered lattice models, *Phys. Rev. A* **99**, 042117 (2019).
- [23] D. J. Thouless, Bandwidths for a quasiperiodic tight-binding model, *Phys. Rev. B* **28**, 4272-4276 (1983).
- [24] Y. Wang, C. Cheng, X.-J. Liu, D. Yu, Many-Body Critical Phase: Extended and Nonthermal, *Phys. Rev. Lett.* **126** 080602 (2021).
- [25] A. Štrkalj, E. V. H. Doggen, I. V. Gornyi, O. Zilberberg, Many-body localization in the interpolating Aubry-André-Fibonacci model, *Phys. Rev. Research* **3**, 033257 (2021).
- [26] S. Xu, X. Li, Y.-T. Hsu, B. Swingle and S. Das Sarma, Butterfly effect in interacting Aubry-Andre model: Thermalization, slow scrambling, and many-body localization, *Phys. Rev. Research* **1**, 032039 (2019).
- [27] V. Mastropietro, Localization of Interacting Fermions in the Aubry-André Model, *Phys. Rev. Lett.* **115**, 180401 (2015).
- [28] S.-X. Zhang and H. Yao, Universal Properties of Many-Body Localization Transitions in Quasiperiodic Systems, *Phys. Rev. Lett.* **121**, 206601 (2018).
- [29] L. Morales-Molina, E. Doerner, C. Danieli and S. Flach, Resonant extended states in driven quasiperiodic lattices: Aubry-Andre localization by design, *Phys. Rev. A* **90**, 043630 (2014).
- [30] E. Bairey, G. Refael and N. H. Lindner, Driving induced many-body localization, *Phys. Rev. B* **96**, 020201 (2017).
- [31] K. S. C. Decker, C. Karrasch, J. Eisert and D. M. Kennes, Floquet Engineering Topological Many-Body Localized Systems, *Phys. Rev. Lett.* **124**, 190601 (2020).
- [32] R. Modak and D. Rakshit, Many-body dynamical phase transition in a quasiperiodic potential, *Phys. Rev. B* **103**, 224310 (2021).
- [33] C. Yang, Y. Wang, P. Wang, X. Gao and S. Chen, Dynamical signature of localization-delocalization transition in a one-dimensional incommensurate lattice, *Phys. Rev. B* **95**, 184201 (2017).
- [34] A. Sinha, M. M. Rams, and J. Dziarmaga, Kibble-Zurek mechanism with a single particle: Dynamics of the localization-delocalization transition in the Aubry-André model, *Phys. Rev. B* **99**, 094203 (2019).
- [35] Y. Ashida, Z. Gong, and M. Ueda, Non-Hermitian physics, *Adv. Phys.* **69**, 249 (2021).
- [36] S. Yao, and Z. Wang, Edge States and Topological Invariants of Non-Hermitian Systems, *Phys. Rev. Lett.* **121**, 086803 (2018).
- [37] F. Song, S. Yao and Z. Wang, Non-Hermitian Skin Effect and Chiral Damping in Open Quantum Systems, *Phys. Rev. Lett.* **123**, 170401 (2019).
- [38] N. Okuma, K. Kawabata, K. Shiozaki and M. Sato, Topological Origin of Non-Hermitian Skin Effects, *Phys. Rev. Lett.* **124**, 086801 (2020).
- [39] K. Kawabata, M. Sato and K. Shiozaki, Higher-order non-Hermitian skin effect, *Phys. Rev. B* **102**, 205118 (2020).
- [40] D. S. Borgnia, A. J. Kruchkov and R.-J. Slager, Non-Hermitian Boundary Modes and Topology. *Phys. Rev. Lett.* **124**, 056802 (2020).
- [41] S. Longhi, Unraveling the non-Hermitian skin effect in dissipative systems, *Phys. Rev. B* **102**, 201103 (2020).
- [42] Y. Fu, J. Hu and S. Wan, Non-Hermitian second-order skin and topological modes, *Phys. Rev. B* **103**, 045420 (2021).
- [43] J. S. Liu, Y. Z. Han and C. S. Liu, A new way to construct topological invariants of non-Hermitian systems with the non-Hermitian skin effect, *Chin. Phys. B* **29**, 010302 (2020).

- [44] W.-T. Xue, Y.-M. Hu, F. Song, Z. Wang, Non-Hermitian Edge Burst, *Phys. Rev. Lett.* **128**, 120401 (2022).
- [45] R. El-Ganainy, K. G. Makris, M. Khajavikhan, Z. H. Musslimani, S. Rotter and D. N. Christodoulides, Non-Hermitian physics and PT symmetry, *Nat. Phys.* **14**, 11 (2018).
- [46] C. M. Bender and S. Boettcher, Real Spectra in Non-Hermitian Hamiltonians Having PT Symmetry, *Phys. Rev. Lett.* **80**, 5243-5246 (1998).
- [47] A. Mostafazadeh, Pseudo-Hermiticity versus PT symmetry: The necessary condition for the reality of the spectrum of a non-Hermitian Hamiltonian, *J. Math. Phys.* **43**, 205-214 (2001).
- [48] R. Shen and C. H. Lee, Non-Hermitian skin clusters from strong interactions, arXiv, 2107.03414 (2021).
- [49] D. V. Novitsky, D. Lyakhov, D. Michels, D. Redka, A. A. Pavlov, and A. S. Shalin, Controlling wave fronts with tunable disordered non-Hermitian multilayers, *Sci. Rep.* **11**, 4790 (2021).
- [50] S. Zhang, L. Jin, and Z. Song, Topology of a parity-time symmetric non-Hermitian rhombic lattice, *Chin. Phys. B* **31**, 010312 (2022).
- [51] F. K. Kunst, E. Edvardsson, J. C. Budich, and E. J. Bergholtz, Biorthogonal Bulk-Boundary Correspondence in Non-Hermitian Systems, *Phys. Rev. Lett.* **121**, 026808 (2018).
- [52] E. J. Bergholtz, J. C. Budich, and F. K. Kunst, Exceptional topology of non-Hermitian systems, *Rev. Mod. Phys.* **93**, 015005 (2021).
- [53] L. Xiao, D. Qu, K. Wang, H.-W. Li, J.-Y. Dai, B. Dóra, M. Heyl, R. Moessner, W. Yi, and P. Xue, Non-Hermitian Kibble-Zurek Mechanism with Tunable Complexity in Single-Photon Interferometry, *PRX Quantum* **2**, 020313 (2021).
- [54] L.-J. Zhai and S. Yin, Out-of-time-ordered correlator in non-Hermitian quantum systems, *Phys. Rev. B*, **102**, 054303 (2020).
- [55] N. Hatano and D. R. Nelson, Non-Hermitian delocalization and eigenfunctions, *Phys. Rev. B* **58**, 8384-8390 (1998).
- [56] S. Longhi, Metal-insulator phase transition in a non-Hermitian Aubry-André-Harper model, *Phys. Rev. B* **100**, 125157 (2019).
- [57] S. Longhi, Spectral deformations in non-Hermitian lattices with disorder and skin effect: A solvable model, *Phys. Rev. B* **103**, 144202 (2021).
- [58] H. Jiang, L.-J. Lang, C. Yang, S.-L. Zhu and S. Chen, Interplay of non-Hermitian skin effects and Anderson localization in nonreciprocal quasiperiodic lattices, *Phys. Rev. B* **100**, 054301 (2019).
- [59] A. Jazaeri and I. I. Satija, Localization transition in incommensurate non-Hermitian systems, *Phys. Rev. E* **63**, 036222 (2001).
- [60] P. Wang, L. Jin and Z. Song, Non-Hermitian phase transition and eigenstate localization induced by asymmetric coupling, *Phys. Rev. A* **99**, 062112 (2019).
- [61] L.-J. Zhai, S. Yin and G.-Y. Huang, Many-body localization in a non-Hermitian quasiperiodic system, *Phys. Rev. B* **102**, 064206 (2020).
- [62] L.-J. Zhai, G.-Y. Huang and S. Yin, Cascade of the delocalization transition in a non-Hermitian interpolating Aubry-André-Fibonacci chain, *Phys. Rev. B* **104**, 014202 (2021).
- [63] L.-Z. Tang, G.-Q. Zhang, L.-F. Zhang and D.-W. Zhang, Localization and topological transitions in non-Hermitian quasiperiodic lattices, *Phys. Rev. A* **103**, 033325 (2021).
- [64] X. Cai, Boundary-dependent self-dualities, winding numbers, and asymmetrical localization in non-Hermitian aperiodic one-dimensional models, *Phys. Rev. B* **103**, 014201 (2021).
- [65] X. Cai, Anderson localization and topological phase transitions in non-Hermitian Aubry-André-Harper models with p-wave pairing, *Phys. Rev. B* **103**, 214202 (2021).
- [66] L.-M. Chen, Y. Zhou, S.A. Chen, P. Ye, Quantum entanglement of non-Hermitian quasicrystals, *Phys. Rev. B* **105**, L121115 (2022).
- [67] I. Y. Goldsheid and B. A. Khoruzhenko, Distribution of Eigenvalues in Non-Hermitian Anderson Models, *Phys. Rev. Lett.* **80**, 2897-2900 (1998).
- [68] Y. Liu, Y. Wang, X.-J. Liu, Q. Zhou and S. Chen, Exact mobility edges, PT-symmetry breaking, and skin effect in one-dimensional non-Hermitian quasicrystals, *Phys. Rev. B* **103**, 014203 (2021).
- [69] Y. Liu, Q. Zhou and S. Chen, Localization transition, spectrum structure, and winding numbers for one-dimensional non-Hermitian quasicrystals, *Phys. Rev. B*, **104**, 024201 (2021).
- [70] T. Liu, H. Guo, Y. Pu and S. Longhi, Generalized Aubry-André self-duality and mobility edges in non-Hermitian quasiperiodic lattices, *Phys. Rev. B* **102**, 024205 (2020).
- [71] C.-X. Guo, C.-H. Liu, X.-M. Zhao, Y. Liu, and S. Chen, Exact Solution of Non-Hermitian Systems with Generalized Boundary Conditions: Size-Dependent Boundary Effect and Fragility of the Skin Effect, *Phys. Rev. Lett.* **127**, 116801 (2021).
- [72] X. Xia, K. Huang, S. Wang, and X. Li, Exact mobility edges in the non-Hermitian t_1-t_2 model: Theory and possible experimental realizations, *Phys. Rev. B* **105**, 014207 (2022).
- [73] S.-B. Zhang, M. M. Denner, T. Bzdušek, M. A. Sentef, and T. Neupert, Symmetry breaking and spectral structure of the interacting Hatano-Nelson model, arXiv, 2201.12653 (2022).
- [74] W. Han and L. Zhou, Dimerization-induced mobility edges and multiple reentrant localization transitions in non-Hermitian quasicrystals, *Phys. Rev. B* **105**, 054204 (2022).
- [75] L. Zhou and Y. Gu, Topological delocalization transitions and mobility edges in the nonreciprocal Maryland model, *J. Phys. Condens. Matter* **34**, 115402 (2022).
- [76] K. Suthar, Y.-C. Wang, Y.-P. Huang, H.-H. Jen, and J.-S. You, Non-Hermitian Many-Body Localization of Coupled Hatano-Nelson Chains, arXiv, 2202.12675 (2022).
- [77] C. Wu, J. Fan, G. Chen, and S. Jia, Non-Hermiticity-induced reentrant localization in a quasiperiodic lattice, *New J. Phys.* **23**, 123048 (2021).
- [78] T. Orito and K.-I. Imura, Unusual wave-packet spreading and entanglement dynamics in non-Hermitian disordered many-body systems, *Phys. Rev. B* **105**, 024303 (2022).
- [79] L. Zhou and W. Han, Non-Hermitian quasicrystal in dimerized lattices, *Chin. Phys. B* **30**, 100308 (2021).

- [80] X.-P. Jiang, Y. Qiao, and J.-P. Cao, Mobility edges and reentrant localization in one-dimensional dimerized non-Hermitian quasiperiodic lattice, *Chin. Phys. B* **30**, 097202 (2021).
- [81] C. Yuce and H. Ramezani, Coexistence of extended and localized states in one-dimensional non-Hermitian Anderson model, arXiv, 2203.02129 (2022).
- [82] H. Markum, R. Pullirsch, T. Wettig, Non-Hermitian Random Matrix Theory and Lattice QCD with Chemical Potential, *Phys. Rev. Lett.* **83**, 484-487 (1999).
- [83] K. Kawabata and S. Ryu, Nonunitary Scaling Theory of Non-Hermitian Localization, *Phys. Rev. Lett.* **126**, 166801 (2021).
- [84] R. Hamazaki, K. Kawabata and M. Ueda, Non-Hermitian Many-Body Localization, *Phys. Rev. Lett.* **123**, 090603 (2019).
- [85] C.M. Dai, Y. Zhang, X.X. Yi, Dynamical localization in non-Hermitian quasicrystals, *Phys. Rev. A* **105**, 022215 (2022).
- [86] L. Zhou, Floquet engineering of topological localization transitions and mobility edges in one-dimensional non-Hermitian quasicrystals, *Phys. Rev. Research* **3**, 033184 (2021).
- [87] Z. Xu, H. Huangfu, Y. Zhang and S. Chen, Dynamical observation of mobility edges in one-dimensional incommensurate optical lattices, *New J. Phys.* **22**, 013036 (2020).
- [88] Z. Xu, S. Chen, Dynamical evolution in a one-dimensional incommensurate lattice with \mathcal{PT} symmetry, *Phys. Rev. A* **103**, 043325 (2021).
- [89] J. Bauer, T.M. Chang, J.L. Skinner, Correlation length and inverse-participation-ratio exponents and multifractal structure for Anderson localization, *Phys. Rev. B* **42**, 8121-8124, (1990).
- [90] Y.V. Fyodorov, A.D. Mirlin, Analytical derivation of the scaling law for the inverse participation ratio in quasi-one-dimensional disordered systems, *Phys. Rev. Lett.* **69**, 1093-1096 (1992).
- [91] S. Yin, G.-Y. Huang, C.-Y. Lo, and P. Chen, Kibble-Zurek Scaling in the Yang-Lee Edge Singularity, *Phys. Rev. Lett.* **118**, 065701 (2017).
- [92] L.-J. Zhai, G.-Y. Huang and H.-Y. Wang, Pseudo-Yang-Lee Edge Singularity Critical Behavior in a Non-Hermitian Ising Model, *Entropy* **22**, 780 (2020).
- [93] M.E. Fisher, Yang-Lee Edge Behavior in One-Dimensional Systems, *Sup. Prog. Theore. Phys.* **69**, 14 (1980).
- [94] J. C. C. Cestari, A. Foerster, M. A. Gusmão and M. Continentino, Critical exponents of the disorder-driven superfluid-insulator transition in one-dimensional Bose-Einstein condensates, *Phys. Rev. A* **84**, 055601 (2011).
- [95] F. Zhong, Probing criticality with linearly varying external fields: Renormalization group theory of nonequilibrium critical dynamics under driving, *Phys. Rev. E* **73**, 047102 (2006).
- [96] S. Gong, F. Zhong, X. Huang, and S. Fan, Finite-time scaling via linear driving, *New J. Phys.* **12**, 043036 (2010).
- [97] Y. Huang, S. Yin, B. Feng, and F. Zhong, Kibble-Zurek mechanism and finite-time scaling, *Phys. Rev. B* **90**, 134108 (2014).
- [98] R. Monaco, J. Mygind, and R. J. Rivers, Zurek-Kibble Domain Structures: The Dynamics of Spontaneous Vortex Formation in Annular Josephson Tunnel Junctions, *Phys. Rev. Lett.* **89**, 080603 (2002).
- [99] J. R. Anglin and W. H. Zurek, Vortices in the Wake of Rapid Bose-Einstein Condensation, *Phys. Rev. Lett.* **83**, 1707 (1999).
- [100] N. D. Antunes, P. Gandra, and R. J. Rivers, Is domain formation decided before or after the transition? *Phys. Rev. D* **73**, 125003 (2006)
- [101] J. Dziarmaga, Dynamics of a Quantum Phase Transition: Exact Solution of the Quantum Ising Model, *Phys. Rev. Lett.* **95**, 245701 (2005).
- [102] B. Damski and W. H. Zurek, Dynamics of a Quantum Phase Transition in a Ferromagnetic Bose-Einstein Condensate, *Phys. Rev. Lett.* **99**, 130402 (2007).
- [103] A. Chandran, A. Erez, S. S. Gubser, and S. L. Sondhi, Kibble-Zurek problem: Universality and the scaling limit, *Phys. Rev. B* **86**, 064304 (2012).
- [104] L.-J. Zhai, H.-Y. Wang and S. Yin, Hybridized Kibble-Zurek scaling in the driven critical dynamics across an overlapping critical region, *Phys. Rev. B* **97**, 134108 (2018).
- [105] X. Tong, Y.-M. Meng, X. Jiang, C. Lee, G. D. d. M. Neto and G. Xianlong, Dynamics of a quantum phase transition in the Aubry-André-Harper model with p -wave superconductivity, *Phys. Rev. B* **103**, 104202 (2021).